EUROFUSION WPMAT-PR(15) 13864

T. Palacios et al.

Tungsten-vanadium-yttria alloys for fusion power reactors (I): microstructural characterization

Preprint of Paper to be submitted for publication in
International Journal of Refractory Metals and Hard Materials

This work has been carried out within the framework of the EUROfusion Consortium and has received funding from the Euratom research and training programme 2014-2018 under grant agreement No 633053. The views and opinions expressed herein do not necessarily reflect those of the European Commission.

This document is intended for publication in the open literature. It is made available on the clear understanding that it may not be further circulated and extracts or references may not be published prior to publication of the original when applicable, or without the consent of the Publications Officer, EUROfusion Programme Management Unit, Culham Science Centre, Abingdon, Oxon, OX14 3DB, UK or e-mail Publications.Officer@euro-fusion.org

Enquiries about Copyright and reproduction should be addressed to the Publications Officer, EUROfusion Programme Management Unit, Culham Science Centre, Abingdon, Oxon, OX14 3DB, UK or e-mail Publications.Officer@euro-fusion.org

The contents of this preprint and all other EUROfusion Preprints, Reports and Conference Papers are available to view online free at http://www.euro-fusionscipub.org. This site has full search facilities and e-mail alert options. In the JET specific papers the diagrams contained within the PDFs on this site are hyperlinked

Tungsten-vanadium-yttria alloys for fusion power reactors (I): microstructural characterization

T. Palacios[a*], M.A. Monge[b] and J.Y. Pastor[a]
[a] Materials Science Department-CIME, E.T.S. de Ingenieros de Caminos, Canales y Puertos, Universidad Politécnica de Madrid, Spain
[b] Departamento de Física, Universidad Carlos III de Madrid, Spain

Abstract

This study and a second part dedicated to the mechanical characterization provide a better knowledge of tungsten (W)-vanadium (V) alloys reinforced with yttrium oxide (Y_2O_3) particles, which have been scarcely investigated. Two W alloys (W-2 or 4 wt.% V-0.5 wt.% Y_2O_3) and a pure W material processed by powder metallurgy and consolidated by hot isostatic pressing were analysed. Along this part, the microstructure of the materials at room temperature is mainly analysed with a field emission scanning electron microscope.

The densification in the compacts show an increase with the V and Y_2O_3 additions. Porosity is reduced because of the formation of a W-V solid solution and V pools that fill the pores between the grains, although such effect is mainly observed in the W2V0.5Y. The microstructure of pure W is composed of coarse polyhedral grains whereas a few coarse W grains, V pools and a nanostructured area, composed of fine W grains with dispersed Y, form the alloys. In contrast to previously studied W-4wt.% V alloys, the V pools exhibit a reduction in the oxygen content, which prevents the formation of acicular oxide structures. Finally, the refinement of the microstructure induced by the addition of V and Y_2O_3 was analised by electron backscattered diffraction measurements. Pure W is presented in high amounts (around 60% of the volume fraction) of grains over 1 μm and only 2% below 100 nm; in these new alloys, grains smaller than 100 nm represent the 20% whereas the population of micron size is highly reduced to less than 10%.

1. Introduction

Fusion power reactors have an enormous power density that can produce environmentally clean and safe energy for our future needs. Nevertheless, these systems require long-lasting materials capable of resisting the damaging effects of high heat flux and intense radiation released by the long-term operation of the reactor [1]. Tungsten (W), the metal with the highest melting point, is considered a premium candidate for high temperature applications such as Plasma Facing Components (PFCs) or structural applications. However W is limited by its inherent brittleness that compromises the structural applications.

With a ductile-brittle transition temperature between 473-673 K and very dependent on the fabrication route or determination method, the development of new high-performance W-based materials with enhanced mechanical properties and radiation tolerance become necessary. At the moment, the main strategies to ductilize bulk W are the alloying with elements such as Ta, V, Ti to refine the grains down to a nanometric scale or an homogeneous dispersion of reinforcing nanoparticles like Y_2O_3 or La_2O_3 [2-5]. The Mechanical Alloying (MA) followed by sintering at temperatures below grain growth would be the most suitable method to produce a fine-grained Oxide Dispersion-Strengthened (ODS) material which fulfil both conditions [6-9]. The addition of V improves the relative density and features an unique capability to withstand intense neutron irradiation, however this remains theorethical and requires some experimental validation [10]. The addition of ODS Y_2O_3 particles enhances the high temperature strength and creep resistance because it features excellent chemical and thermal stability [11, 12]. Eventhougth a modest progress was achived with the production of new tungsten alloys, at present, developed W-based materials do not satisty the required properties for structural aplications or PFCs for the future reactors under design such as DEMO.

In this study, an extensive microstructural characterization of the produced W-V reinforced alloys was performed using Electron BackScatter Diffraction (EBSD) analysis, which is a powerful technique used for the characterization of local crystallograpic characteristics. Although sample preparation requires some special attention for a reliable analysis, it is a very yielding method that provides many quantitative post-processing results derived from one single analysis such as grain size, grain orientation, local texture or strain and phase identification. The effect of the production route on the microstructure is discussed in terms of solid solution and diffusion phenomena of the vanadium.

2. Materials and samples

A pure W material as reference and two W-based alloys were studied. The alloys had the target composition of W-2 wt.% V-0.5 wt.% Y_2O_3 and W-4 wt.% V-0.5 wt.% Y_2O_3, hereafter referred to as W2V0.5Y and W4V0.5Y, respectively. All materials were prepared by mixing starting powders (Table 1) for 4 h. The powder mixtures then underwent MA inside a sealed WC vessel filled with a high purity Ar atmosphere for 40 h in a high-energy planerary ball mill. Afterwards, the alloyed powders were canned and degassed at 673 K for 24 h under vacuum atmosphere before vacuum sealing. A subsequent Hot Isostatic Pressing (HIP) at 1573 K for 2 h at 195 MPa consolidated the canned powders. Further information about materials processing can be found in Savoini *et al.* [13]. From this fabrication process, we obtained cylinders with dimensions of 30 mm diameter and 50 mm in length that were used for all measurements and analysis.

Table 1
Starting powder properties [13].

Power	Purity (%)	Average particle size (μm)
W	99.9	< 5
V	99.5	< 40
Y_2O_3	99.5	0.01-0.05

3. Experimental methods

To measure the experimental density (ρ_{exp}) of the samples, the Archimedes method using high purity ethanol at room temperature was used. In addition, theoretical density (ρ_{th}) of the alloys W-xV-0.5Y_2O_3 (for x=2 or 4) was calculated using the density of each component and the following formula (1):

$$\rho_{th} = \frac{100 \cdot \rho_W \cdot \rho_V \cdot \rho_{Y_2O_3}}{(100 - x - 0.5)\rho_V \rho_{Y_2O_3} + x\rho_W \rho_{Y_2O_3} + 0.5\rho_W \rho_V} \quad (1)$$

where ρ_x is the density (ρ_W=19.25 g/cm^3, ρ_V=6.11 g/cm^3 and ρ_{Y2O3}=5.03 g/cm^3, respectively) of the corresponding elements in the alloy. Based on these two results (experimental and theoretical densities), relative density (ρ_r) was also calculated to determine the porosity of the materials.

For the microstructural characterization, the samples were examinded in an Auriga column Field Emission Scanning Electron Microscope (FE-SEM) from Zeiss (Germany) equipped with an Energy Dispersive X-ray spectrometer (EDX) and EBSD detector. To perform the microstructural analysis, samples were mechanically polished up to 1 μm diamond suspension and etched with the solution (10 g KOH, 10 g $K_3Fe(CN)_6$ in 100 ml distilled water) for 7 s. Because sample surfaces in EBSD must be free of relief for good quality EBSD patterns and realiable results, a final polishing with colloidal silica was performed as well. Even though this step can be achieved with other methods like electropolishing or ion milling, colloidal silica was used because it is suitable for materials with very high atomic number. The objective of this step was to remove the deformation layer during the mechanical polishing and slightly etch the sample surface. This was done even though sample preparation on materials with a high atomic number is not as critical because they have stronger Kikuchi patterns [14].

After the acquisition, images from the EBSD patterns were reconstructed using the MTex v4.0.16 data analysis software [15]. The applied criterion for discriminating the boundaries was a crystallographic misorientation more than 5° between adjacent crystalline domains. Only results with high percentage of indexed patterns i.e. high image quality were used. This way, it was possible to apply the noise reduction procedure to suppress the zero solution (unindexed patterns) and to conduct reliable microstructural characterization. Otherwise, the presence of many dark pixels (low indexed patterns) led to unreliable characterization. For the grain size measurements a minimum of 1000 complete grains per single map were considered. Great care was taken to identify the grains from the EBSD data analysis, a detailed description of the applied criteria can be found in Mingard et al. [16]. The grain size distribution, meanwhile, was determined from the EBSD measurements from an improved approach of the Johnson-Saltykov stereological method to obtain the spatial grain size distribution of the 3D microstructure from 2D dimensional grain size measurements [17].

4. Results and discussion

4.1 Density

The relative density (ρ_r) of the W2V0.5Y and W4V0.5Y alloys was improved in comparison to pure W (Fig. 1). The porosity was reduced from 8.4% in pure W to 2.6% with the addition of 2V0.5Y. With increasing V content up to 4 wt.%, the resulting porosity increased to 5.4%, but this is still lower than pure W. On the contrary to these results, some previous materials produced by HIP showed a decreased porosity when increasing the V content [18, 19]. Similarly, W alloys consolidated by spark plasma sintering have been reported that exhibited an increase in the densification with linearly increasing V content [20]. This densification was produced because a V-rich phase or pure V fill the pores between grains, even thorugh the W-V phase diagram features complete solubility [21]. This contradictory result may be the consequence of an incomplete solubility of V in the W matrix during the MA process or a segregation of V by diffusion processes during the sintering. Therefore, the decrease in ρ_r for W4V0.5Y versus W2V0.5Y may be the result of a formation of a net of small, interconnected pores during processing. The increase of the V content in the W4V0.5Y alloy, makes more difficult to obtain an homogeneous solid solution of W-V by MA, the powder particles exhibit an homogeneous microstructure, but some small regions are V-enriched [13]. Such regions, are very small in comparison with the V pools observed after sintering. Although the effect of the ODS particles to W does not favour the densification (9.6% porosity for W1Y materials), they do provide other benefits to the alloy such as stabilization of the microstructure at high temperatures [22, 23].

4.2 Micromechanical characterization

Scanning electron micrographs of the materials at low magnification (Fig. 2) reveal the great difference between pure W and W-V-Y_2O_3 alloys. The pure W microstructure is clearly visible under low magnification and consists of a relatively well-mixed equiaxial grains and many intergranular porosity. However, to better understand the microstructure of the W2V0.5Y and W4V0.5Y alloys, further magnification is needed. In spite of this, both alloys exhibit similar microstructures with an increased amount of black areas in the W4V0.5Y alloy that corresponds to the increase in the V content (primarily the larger areas) but also to increasing porosity with respect to W2V0.5Y (Fig. 2, bottom).

For higher magnification (Fig. 3), the W-V based alloys with Y_2O_3 reinforcement exhibit similar microstructure as anticipated. The refined microstructure is composed of a greyish zone with large grains (W grains), black patches (V pools) and a nanostructured area (W-V solid solution). The size and morphology of these black patches were examined along the whole surface during the analysis. It was found that it is indiferrent from the material, because both big and small pools were observed in the two W-V-Y alloys; although there was an obvious increase in the number found in W4V0.5Y because of the higher V content.

The EDS-SEM analysis of the W2V0.5Y alloy (Fig. 4) reveals that the black areas are mainly composed of V pools segregated in the interstices between W particles, whereas W and Y are distributed along the entire surface. Because Y_2O_3 nanoparticles are very finely dispersed, it was not possible to identify them from this analysis and further magnification is needed. Nevertheless, they should be dispersed within the W grains as spheroidal dispersoids of variable size according to our previous study [22]. Although we have calculated a porosity of 2.4 and 5.4% for W2V0.5Y and W4V0.5Y, respectively, it is difficult to distinguish under FE-SEM, or even in the EDX maps.

The presence of acicular structures inside the V pools was previously reported for V alloys in W-4V [19]. They were attributed to the formation of V oxides due to the high solubility of O in V [24], but such structures were not observed in the V pools of these ODS-reinforced alloys.

To confirm the composition of the V pools, an EDX line scan along this area was performed (Fig. 5). The profile shows that the composition of the V pools is composed of more than 90% of V with a slight increase in the oxygen content but not enough to form the acicular structures because they were not observed. This fenomenon was attributed irregularities during the fabrication process or to the influence of Y_2O_3, since the fabrication process is the same as that for previously reported materials.

During the quantitative acquisition of the EBSD data, only information from the W areas were collected because Y is too small and the V pools did not diffract any pattern. This may be due to a mean crystal size smaller than the equipment resolution or because of an amosphous V structure in these pools. Nevertheless, it is not relevant for our purposes. Therefore, when considering the porosity of each material, the analysed volume fraction approximately corresponds to 91.6, 92.2 and 86.8% for pure W, W2V0.5Y and V4V0.5Y, respectively.

Additionally, the volume fraction distribution for each population from reconstructed EBSD data (Fig. 6) confirms the refinement of the grain size for the W-V-Y alloys in accordance with the micrographs. Pure W has 20% of grains with 1 µm size and 40% even larger. Meanwhile, the most probable grain size population for the alloys is considerably smaller, 200 nm, with 12 and 16.5% for W2V0.5Y and W4V0.5Y, respectively. During the analysis, step size was 10 pixels, therefore only grains above 20 nm i.e. min four pixels, are represented. The nanostructured area is clearly observed in the alloys because grains between 20-100 nm have a higher volume fraction, around 20%, than pure W with less than 2%. Coarse grains, around 2.5 µm, are observed in all the materials, although in different fractions: 3, 2, and 1% for pure W, W2V0.5Y and W4V0.5Y, respectively.

5. Conclusions

The effect of adding 2 or 4 wt.% V and 0.5 wt.% Y_2O_3 to pure W produced by mechanical alloying (MA) and hot isostatic pressing (HIP) on the microstructure of the alloys at room temperature is analysed in this paper. The following conclusions can be drawn from the results:

- The addition of the alloying elements produce high densification of the materials; W2V0.5Y alloy have reduced porosity to 2.6% because of the complete solubility of W-V that fill the intergranular pores.
- The microstructure of the alloys is formed by coarse W grains, V pools and a rough nanostructured area. Pools have a composition of more than 90% V with a small amount of O. However, the previously observed acicular oxide structures were not presented.
- Grains size distribution shows grain refinement in the W-V-Y alloys. The mean grain size is highly reduced and a big population of the is smaller than 100 nm.

Acknowledgements

This work has been carried out within the framework of the EUROfusion Consortium and has received funding from the Euratom research and training program 2014-2018 under grant agreement No 633053. The views and opinions expressed herein do not necessarily reflect those of the European Commission. The authors would also like to acknowledge to Ministerio de Economía y Competitividad of Spain projects (MAT2012-38541-C02-02 and ENE2012-39787-C06-05) and Comunidad de Madrid (research project S2013/MIT-2862-MULTIMATCHALLENGE and S2013/MAE-2745-TECHNOFUSION(II)-CM) for funding for this research.

References

[1] P. Norajitra, L.V. Boccaccini, E. Diegele, V. Filatov, A. Gervash, R. Giniyatulin *et al.* J. Nucl. Mater. 329-333 (2004) 1594-1598.
[2] M. Rose, A.G. Balogh, H. Hahn Nucl. Instrum. Methods Phys. Res. B 127 (1997) 119–122.
[3] N. Nita, R. Schaeublin, M. Victoria J. Nucl. Mater. 329 (2004) 953–957.
[4] S.J. Zinkle, J.T. Busby Mater. Today, 12 (2009) 12–19.
[5] O. El-Atwani, A. Suslova, T.J. Novakowski, K. Hattar, M. Efe, S.S. Harilal *et al*. Mater. Charact. 99 (2015) 68-76.
[6] L. Veleva R. Schaeublin, M. Battabyal, T. Plociski, N. Baluc, Int. J. Refrac. Met. Hard Mater. 50 (2015) 210–216.
[7] A. Muñoz , B. Savoini, E. Tejado, M.A. Monge, J.Y. Pastor, R. Pareja J. Nucl. Mater. 455 (2014) 306–310.
[8] M.V. Aguirre, A. Martin, J.Y. Pastor, J. LLorca, M.A. Monge, R. Pareja, J. Nucl. Mater. 404 (2010) 203–209.
[9] M. Mabuchi, K. Okamoto, N. Saito, T. Asahina, T. Igarashi, Mater. Sci. Eng. A 237 (1997) 241–249.
[10] J. Hohe, P. Gumbsch J. Nucl. Mater. 400 (2010) 218-231.
[11] Y. Itoh, Y. Ishiwata JSME International Journal. Series A 39 (1996) 429-434.
[12] V. Swamy, H.J. Seifert, F. Aldinger J. Alloys Compd 269 (1998) 201-207.
[13] B. Savoini, J. martínez, A. Muñoz, M.A. Monge, R. Pareja J. Nucl. Mater. 442 (2013) 229-232.
[14] Y-J. Chen, J. Hjelen, H.J. Roven. Trans. Nonferrous Met. Soc. China 22 (2012) 1801-1809.
[15] F. Bachmann, R. Hielscher, H. Schaeben Ultramicroscopy 111 (2011) 1720-1733.

[16] K.P. Mingard, B. Roebuck, E.G. Bennett, M.G. Gee, H. Nordenstrom, G. Sweetman, P. Chan Int. J. Refract. Met. Hard Mater. 27 (2009) 213-223.
[17] Y.H. Xu, H.C. Pitot Comput. Meth. Prog. Bio. 72 (2003) 1-20.
[18] T. Palacios, J.Y. Pastor, M.V. Aguirre, A. Martin, M.A. Monge, A. Muñoz *et al*. J. Nucl. Mater. 442 (2013) S277-S281.
[19] M.V. Aguirre Comportamiento mecánico de nuevas aleaciones de wolframio en función de la temperatura, PhD tesis, Universidad Politécnica de Madrid, 2014.
[20] K. Arshad, M-Y Zhao, Y. Yuan, Y. Zhang, Z-H Zhao, B. Wang *et al*. J. Nucl. Mater. 445 (2014) 96-100.
[21] ASM Handbook Comitee, ASM Handbook: Alloy Phase diagrams, vol. 03, ASM 1992.
[22] T. Palacios, A. Jimenez, A. Muñoz, M.A. Monge, C. Ballesteros, J.Y. Pastor J. Nucl. Mater. 454 (2014) 455-461.
[23] T. Palacios, J.Y. Pastor Submitted to J. Nucl. Mater.
[24] D.G. Alexander and O.N. Carlson Metall. Trans. 2 (1971) 2805-2811.

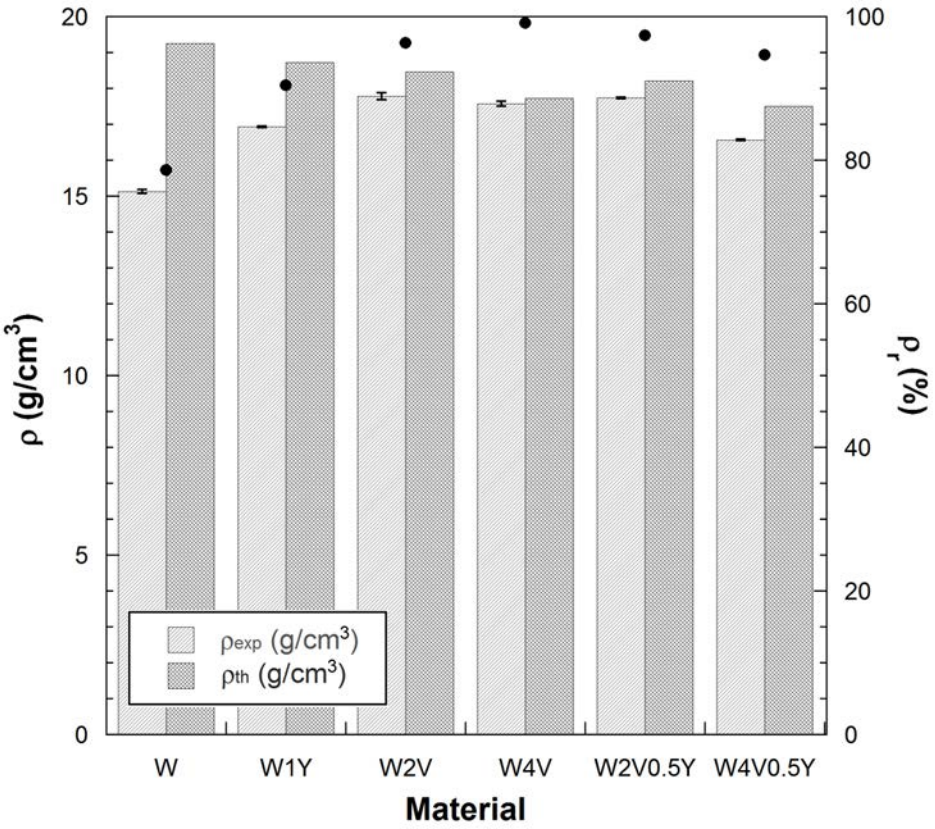

Fig. 1 Experimental density (ρ_{exp}), theoretical density (ρ_{th}) and relative density (ρ_r) for W2V0.5Y and W4V0.5Y alloys. The figure also shows previously reported results for pure W, W1Y [18], W4V [22] and W2V (unpublished data) for comparison of these new values. Standard error bars are also presented for ρ_{exp} and ρ_r but they are inappreciable in some cases because of the very low values.

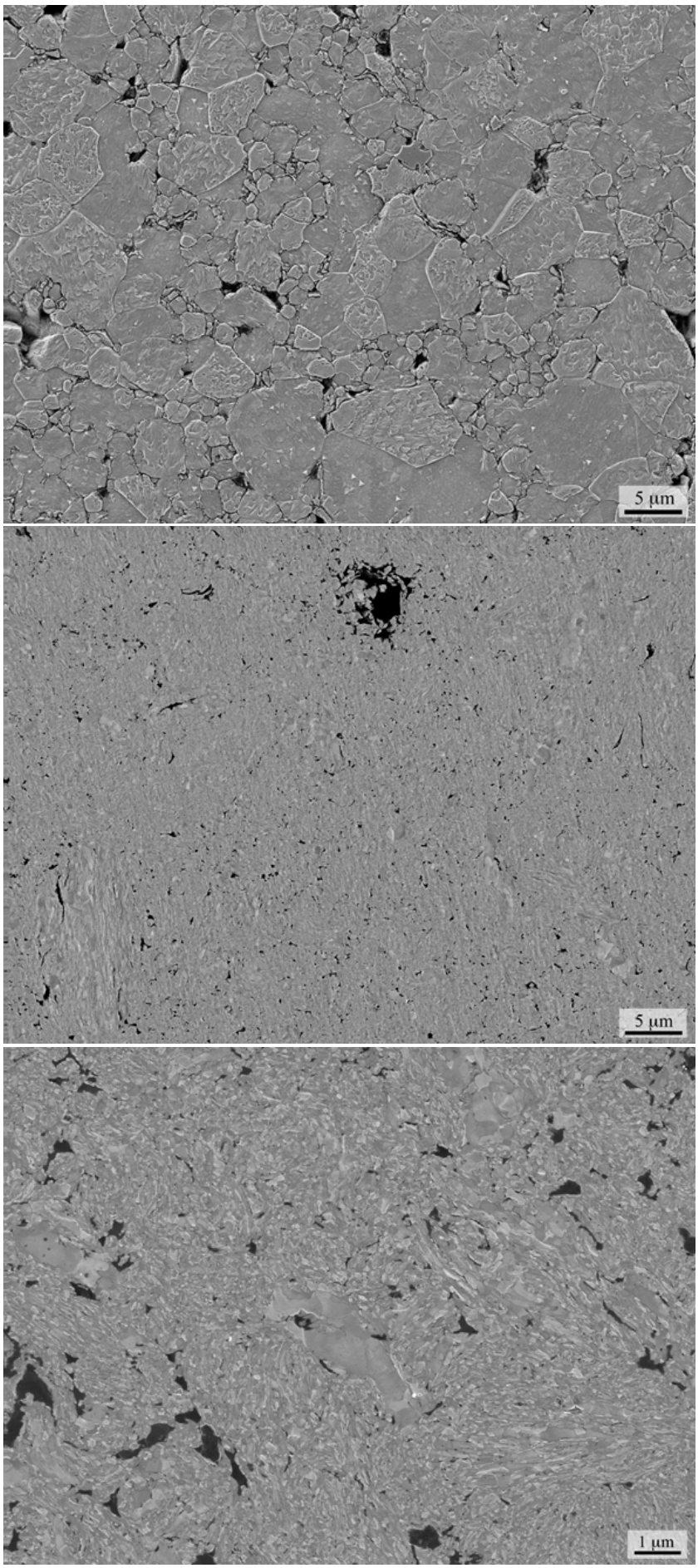

Fig. 2 Micrographs for pure W (upper), W2V0.5Y (middle) and W4V0.5Y (bottom) at 300 K.

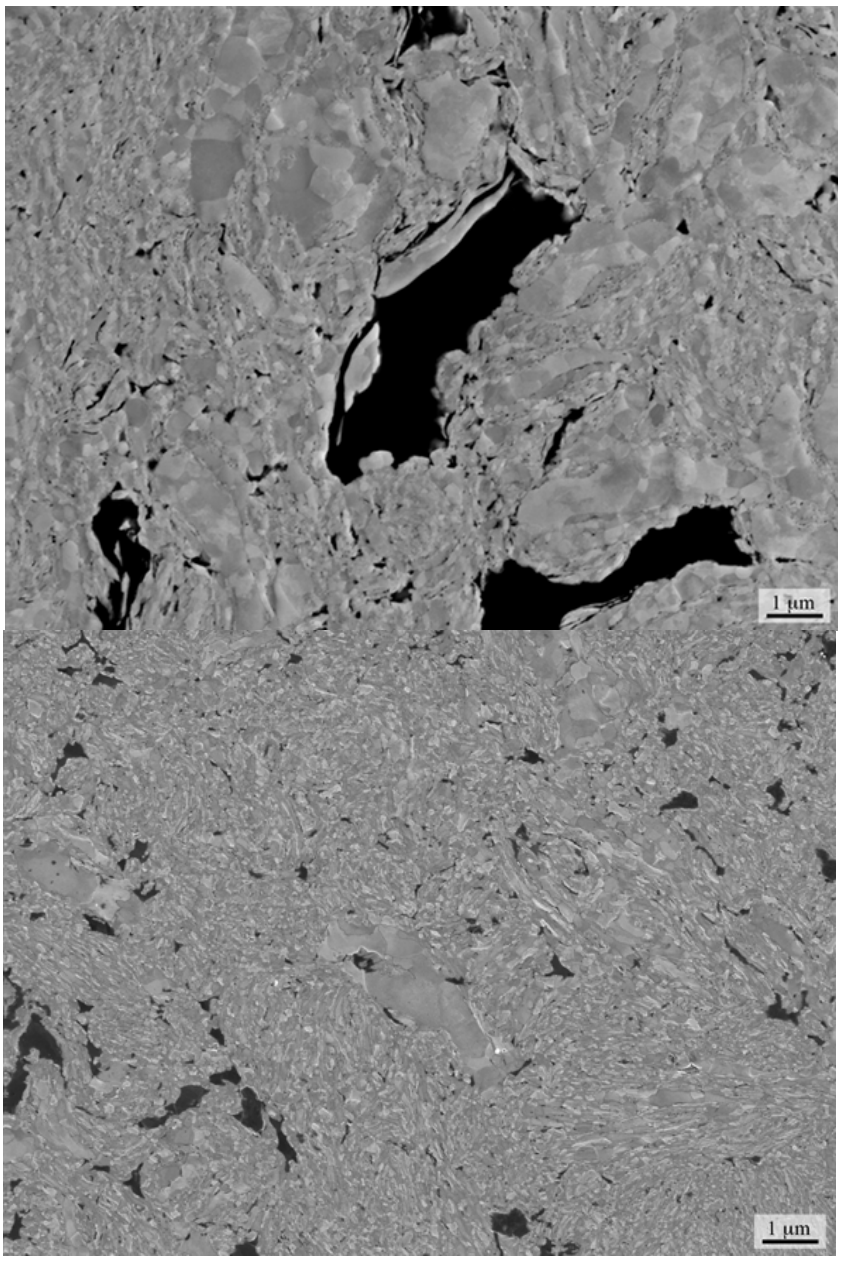

Fig. 3 Micrographs for W2V0.5Y (upper) and W4V0.5Y (bottom). The V pools and the rough nanostructured area can be clearly distinguished.

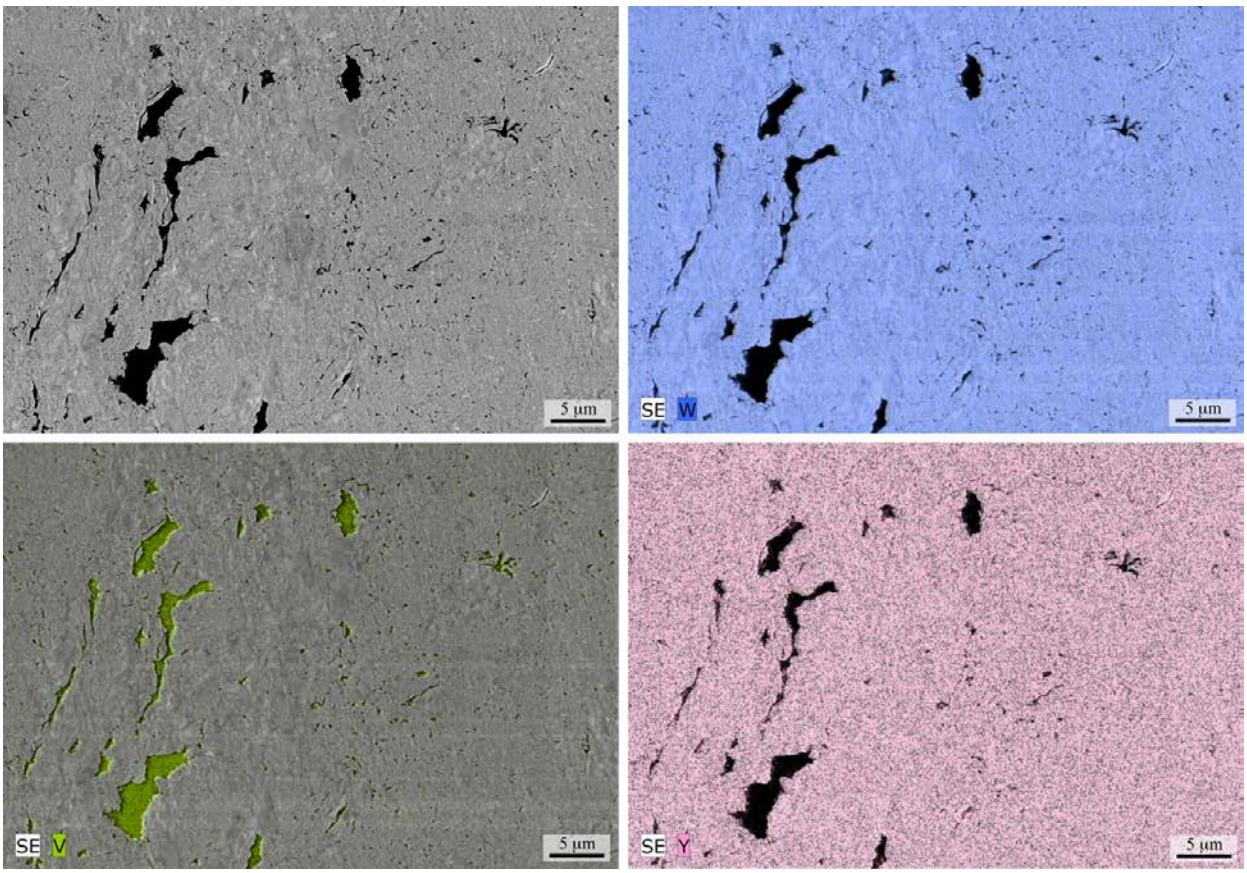

Fig. 4 EDX compositional mapping for W2V0.5Y at 300 K. W4V0.5Y alloy exhibited similar morphology.

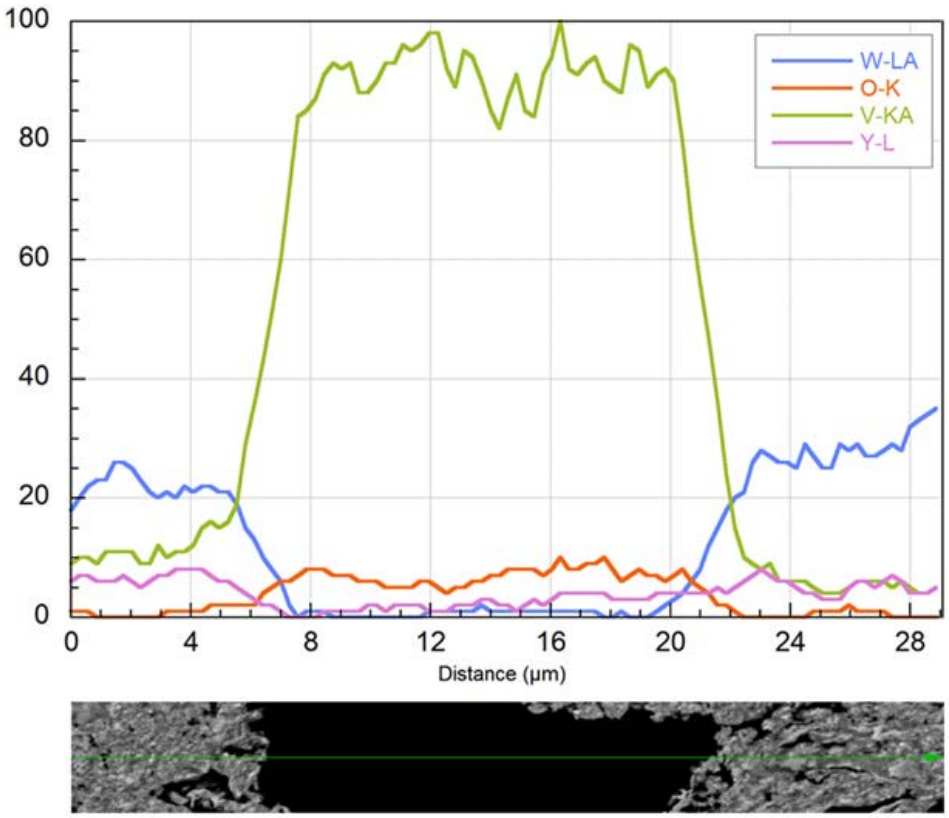

Fig. 5 EDX linescan showing the profile content for a V pool of the W4V0.5Y alloy.

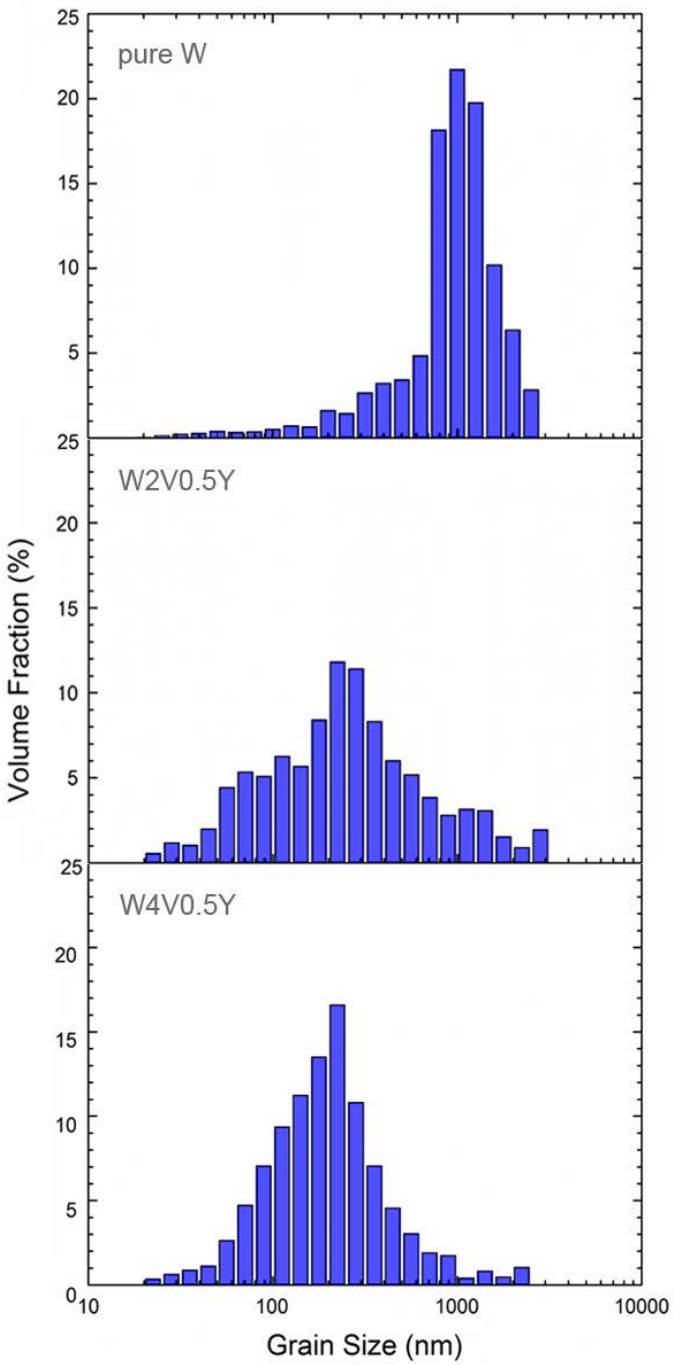

Fig. 6 Histogram of circle equivalen grain size distribution for pure W (upper), W2V0.5Y (middle) and W4V0.5Y (bottom).

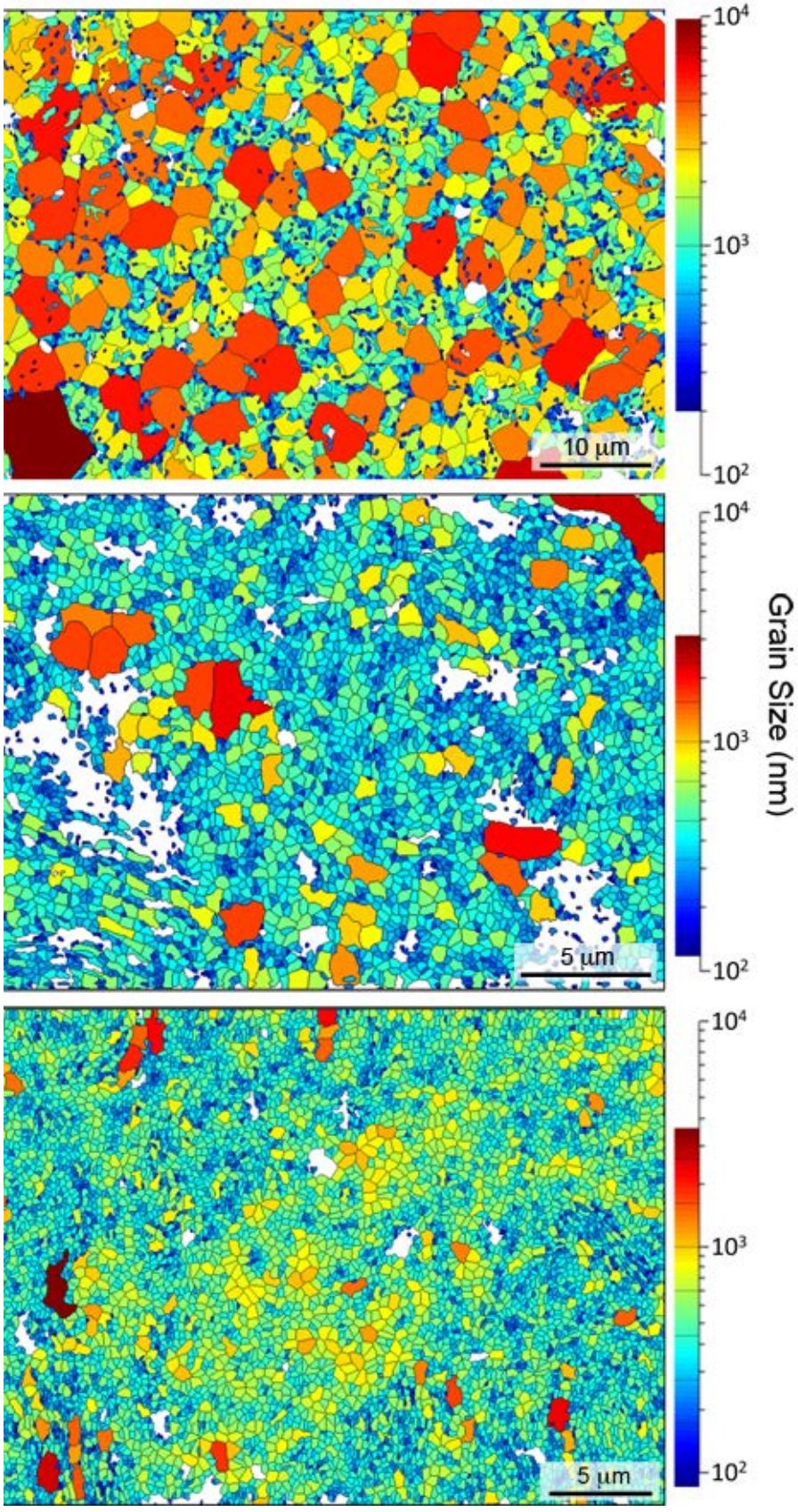

Fig. 7 EBSD measured W grains coloured as a function of their cicle equivalent diameter for pure W (upper), W2V0.5Y (middle) and W4V0.5Y (bottom). White regions correspond to cavities or V-rich regions.